Modified Rodriguez Parameters based Non Linear Disturbance Observer Control of Quadrotor for Aggressive Flights

Patanjali Maithani
Netaji Subhas University of Technology

Dr.Vijyant Agarwal
Netaji Subhas University of Technology

***Abstract*—For aggressive acrobatic maneuvers of quad rotors, it is essential to have quick and precise control. This paper presents a systematic approach to achieve the same using the cascade control approach. We have discussed the design of both the inner and outer loop controller with their stability proof. We have designed an inner-loop non-linear PID control law that tracks the fast time-varying set-points, generated by the outer loop, based upon the errors between the actual and desired trajectory. A Non-linear Disturbance observer is employed to make the controller robust to the exogenous disturbances existing in the surrounding. We have used the Modified Rodriguez Parameters (MRPs) to represent the quad rotor's orientation, which solves the unwinding as well as singularity problem using a switching strategy that is computationally efficient. The ease nature of handling singularity in MRPs enables us to have a robust global full degree of freedom, discontinuous trajectory tracking control. Additionally, we have implemented an MRP based Extended Kalman Filter(EKF) for estimating the attitude and compensating for the measurement error from the sensors, and uncertainty in the system. An algorithm for handling the up-down orientation of the quadrotor at the start of the flight has also been developed. Finally, numerical simulation results illustrate the efficacy of the proposed control strategy for achieving aggressive flights.**

***Index Terms*—Quadrotor, Attitude estimation, and control, MRP-based Extended Kalman Filter, Non-linear Disturbance Observer, NON-linear PID, PD**

I. Introduction

There are many fields where quadrotors have been a great aid like in inspection, mapping, surveying, delivering, surveillance, agriculture, and, most importantly, military. As we aim to have a complete autonomous action of the quadrotor, we must take into consideration all the absurd situations that may occur during flight. One of those situations could be of an obstacle instantly coming in front of the quadrotor out of nowhere. In the case of indoor environments like a house, office buildings, there is very little space available for the quadrotor to maneuver. In these situations, the quadrotor should have the ability to execute sharp turns quickly. Thus a quick responding attitude controller is required, which can make the quadrotor achieve its desired orientation in the least time. In a quadrotor, there are generally two control loops, the outer one defines the reference signal to the inner one in terms of desired orientation trajectory by considering the error between the desired and the actual 3d-space trajectory, and the internal control loop functions to achieve the desired attitude signal received from the outer loop. Thus, forming a cascaded control approach. Attitude control is the most vital control system to achieve the desired position and desired velocity of the quadrotor, without it, the quadrotor won't be able to follow its desired trajectory in a highly dynamic and uncertain environment.

During the literature survey, various control strategies were studied. References [18],[26],[1],[28] are based upon sliding mode control law, references[20] ,[27] designed backstepping controllers and [25],[17] designed control laws using Lyapunov functions. An MRP based Lyapunov control law for attitude tracking is given in[25]. In [17], the author, along with MRP based Lyapunov control law also considers the saturation of actuators in the design of control law. Reference [14] provides a survey of various kinds of controllers, both linear and non-linear types, used in quadrotor. Controllers that do not account for the disturbances and uncertainty are prone to trajectory tracking errors. References [7],[18],[30],[6],[19],[26],[22] provides various kinds of disturbance estimating techniques with simulations verifying them. In our paper, based upon the formulation of[9], we have designed a non-linear disturbance observer to counter the effect of unknown disturbances in the environment and have a finite time convergence. In [7], the author has employed an IMU-based disturbance estimation model using a second-order filter to track the disturbance in the first half of the round trip and then has used it in the second half as the feedforward compensation term in the cascade PD control law. Their strategy has resulted in the time decrement of the total flight. In [1], the author has designed a Sliding Mode control law while considering the effect of parametric uncertainties in the model parameters, and disturbances in the surroundings. They have employed a non-linear disturbance observer to estimate and reject the disturbances. In [16], the author has used quaternions to form the uncertainty and disturbance estimator(UDE)-based control law for achieving singularity free tracking. A virtual control law designed by them handles the problem associated with unwinding phenomena. Unwinding problem occurs when the quadrotor makes the longer rotation, instead of the shorter one, to attain the desired orientation.References[1],[8],[11] provides solutions to the unwinding problem with quaternions. To have a time-scale separation between the outer and inner loop, the author in [16] has designed a quaternion-based non-linear reference model for generating set points for inner loop. A similar approach with MRPs is present in our paper, where a command filter generates reference signals for the attitude controller. Unwinding problem, in the case of MPPs, is avoided by using the non-uniqueness property of the MRPs. In MRPs, there exist two sets of parameters for a specific orientation,

original and shadow set MRPs. Switching between them as the norm of one exceeds unity, which refers to 180-degree rotation about the principal axis, will solve the unwinding problem, and will also avoid the singular point, which is 2π and 0 for MRPs and shadow set MRPs, respectively.

In [15], Euler angles represent the orientation of the quadrotor, and the mathematical model of the quadrotor used to form the disturbance estimator contains many transcendental functions, which results in high computational cost. Euler angle parmeters faces the problem of gimbal lock and therefore large angle maneuvers are not possible. In [19], Unscented Kalman Filter(UKF) based disturbance estimator estimates the external disturbance. The advantage of using UKF instead of EKF is that it doesn't involve the calculation of jacobian, but the method gets computationally heavy when the number of sigma points increases. In [6], the author has used a mechanical approach to counterbalance the disturbances using an angular momentum wheel. A quadrotor estimates its state using onboard sensors like magnetometer, accelerometer, and gyroscopes. These sensors don't directly measure the state of the quadrotor. Their measurements are further processed to get an estimate. According to the precision these sensors offer in their readings, prices of these sensors vary from low to high. A system like a quadrotor generally works with low-cost sensors. The sources of these noises are likely because of the vibratory nature of motors in the system, which disturbs accelerometer reading, magnetic disturbance due to electronics onboard, which perturbs the magnetometer readings. Gyroscopes measurement is supposed to be integrated over time to track the orientation, but due to noisy measurements after a series of integration steps, the estimate experiences a drift known as gyro drift. Extended Kalman filter fuses measurements from these different sensors to achieve a better state-estimate than the individual sensor alone. The use of the Modified Rodrigues Vector has proven useful in the development of Extended Kalman Filters for attitude estimation because it reduces the length of the state vector, and there is no need to enforce the unit length constraint as for the quaternion [5]. The quaternion normalization constraint produces a singularity in the Kalman filter covariance matrix [10]. Refference[2] discusses this problem with quaternions and explains the solution to it based upon the manifold theory. For determining the attitude of a rigid body, it's essential to know the information of at least two non-collinear vectors in the body frame and the inertial frame of reference (Whabas problem). In the case of the quadrotor, one non-collinear vector is the gravity vector measured by the accelerometer, and the other non-collinear vector is the magnetic vector measured by the magnetometer. Methods like TRIAD, Davenport's q-method, QUEST, and OLAE solve this kind of problem. Reference [5] provides an MRP-based algorithm to address the same problem. Once the attitude at a single point(time instance) is known, using the algorithm discussed in [5], the Extended Kalman filter is employed on series of such measurements, along with gyroscope measurements to compensate for the measurement errors of the sensors and to reach out to a better estimate. In [10], the author describes the MRP-based EKF implementation but doesn't provide the mapping for the transformation of the state error covariance matrix when switching to shadow set MRPs occurs. In [13],[24], the authors provide the mapping function for the same. In our paper, we have implemented the same design of MRP-based EKF as given in [24]. Although the EKF algorithm performs well for compensating uncertainty and noises in the system and measurements, its performance is dependent on the initial guesses of noise covariance matrices. Their poor definition can lead to inaccurate estimation as well as divergence and stability problems [23]. Reference[23] provides a method to identify these covariance matrices to improve orientation estimation. There are several other parameterizations other than MRPs to represent the orientation of a rigid body like Euler angles, quaternions, Direction cosine matrix, Cayley Klein parameters, Rodrigues parameter. Reference [29] provides derivations of kinematic equations, advantages, disadvantages, and related algebraic expressions to all these parameterizations. In this paper, we have used MRPs, as they are the minimal representation of the attitude, and singularity avoidance by just switching to shadow set MRPs is very handy. It is stated in the reference [3] that there cannot exist a continuous vector field on a compact manifold that has a globally asymptotically stable equilibrium point. In our control law, the switching between the MRPs and shadow set MRPs makes the control law discontinuous and allows for attaining a globally asymptotic stability. The remaining part of the paper is as follows: Section II describes the MRPs and the quadrotor model. Section III explains the MRP-based Extended Kalman filter. In Section IV, a Non-linear disturbance observer is derived based on the dynamic model of the quadrotor. In section V, the derivation of inner and outer loop control laws with their stability analysis is given. After that, in Section VI, we have proposed an algorithm for improving the convergence time when the quadrotor is left initially at an up-down orientation. . At last, section VII provides the results of numerical simulations for the described approach.

II. Quadrotor model

The quadrotor is a coupled system with highly non-linear dynamics. It consists of four propellers, driven by motors, which vary their angular speeds to produce varying thrusts and moments to generate accelerations along and about x,y, and z axes, respectively, of body frame β. The Quadrotor system, is an under-actuated system for having a degree of freedom of six and control inputs as four. Due to which, its roll and pitch motion accompany a translation motion also. The coordinate systems used for developing the quadrotor is shown in Fig.1 . As stated by Euler, any rotation of a rigid body is equivalent to a single rotation about a particular fixed axis called the Euler axis.Based on this, the MRPs, $\sigma \in \Re^3$, can be defined as

$$\sigma = \hat{n} \tan(\frac{\phi}{4}) \tag{1}$$

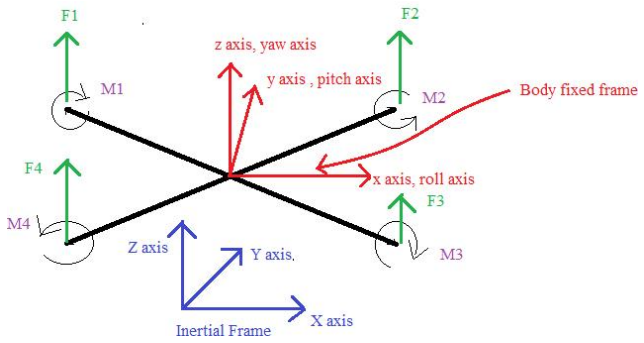

Fig. 1. Representation of the quadrotor model with frame of reference.

where $\phi$is the magnitude of rotation and $\hat{n}$is the principal axis of rotation. The shadow set MRPs are defined as

$$\sigma^s = \frac{-\sigma}{\sigma^T\sigma} \tag{2}$$

The kinematic equation of MRPs can be written as

$$\dot{\sigma} = G(\sigma)\omega \tag{3}$$

$$G(\sigma) = \left(\frac{1}{4}\right)\left[(1-\sigma^T\sigma)_3 + 2S(\sigma) + 2\sigma\sigma^T\right] \tag{4}$$

where $\omega \in \Re^3$is the angular velocity of the quadrotor expressed in body frame β and $S(\sigma)$refers to cross product expression as $a \times b = S(a)b$, where

$$S(\sigma) = \begin{bmatrix} 0 & -\sigma_3 & \sigma_2 \\ \sigma_3 & 0 & -\sigma_1 \\ -\sigma_2 & \sigma_1 & 0 \end{bmatrix} \tag{5}$$

Relation between MRPs and rotation matrix is given by the following equation

$$R = I_3 - \frac{4(1-\sigma^T\sigma)}{(1+\sigma^T\sigma)^2}S(\sigma) + \frac{8}{(1+\sigma^T\sigma)^2}S(\sigma)^T S(\sigma) \tag{6}$$

where R matrix rotates a vector from inertial frame to body frame. As given in Fig 1, there are two frames of reference, one is on the body of the quadrotor, and the other one, the inertial frame, is fixed on the Earth. The position and the velocity of the quadrotor in the inertial frame I are $P = [x, y, z]^T$ $v = [\dot{x}, \dot{y}, \dot{z}]^T$ and thus, the translation dynamic and kinematic equations are as follows

$$\dot{p} = v \tag{7}$$

$$\dot{v} = -ge_3 + \frac{f_B}{m}R^T e_3 + \frac{d}{m} \tag{8}$$

$$f_B = \sum_{i=1}^{4} F_i$$

$$f_I = \frac{f_B}{m}R^T e_3$$

where, $e_3 = [0, 0, 1]^T$, F_i represents the thrust force generated by each propeller,$f_i$represents the translational force in an inertial frame . Also,the net thrust force f_b is acting along the Zaxis of the body frame ,R^Trepresents the rotation from body frame β to inertial frame I, g is the gravitational acceleration, and m is the mass of the quadrotor. Considering $J \in \Re^3$ as the principal inertia matrix of the quadrotor frame w.r.t the body frame,$\tau = [\tau_1, \tau_2, \tau_3]^T$ as the control torque about the x,y and z axes of the body frame β, and $\omega = [\omega_1, \omega_2, \omega_3]^T$as the angular velocity of the quadrotor w.r.t the inertial frame expressed in the body frame, the rotational dynamics of the quadrotor system can be written as

$$\dot{\omega} = J^{-1}(-S(\omega)J\omega + \tau) + J^{-1}(\tau_d) \tag{9}$$

where τ_d is the torque due to exogenous disturbances. Control torque and net thrust are related to individual motor's thrust by the following relation

$$\begin{pmatrix} f_b \\ \tau_1 \\ \tau_2 \\ \tau_3 \end{pmatrix} = \begin{bmatrix} 1 & 1 & 1 & 1 \\ d & d & -d & -d \\ d & -d & -d & d \\ c & -c & c & -c \end{bmatrix} \begin{pmatrix} F_1 \\ F_2 \\ F_3 \\ F_4 \end{pmatrix} \tag{10}$$

where d is the distance of the perpendicular drawn from the centre of the quadrotor to the line joining any two adjacent motors, and c is the moment-force coefficient.

III. MRP-EKF Implementation

Camera and GPS sense position and velocity of the quadrotor in indoor and outdoor environments, respectively. In this paper, we consider implementing EKF to IMU measurements only, for estimating orientation and angular velocity. For state,$X = [\sigma, \omega]^T$, the state dynamic of rotational motion with white gaussian noise can be written as

$$\dot{X} = f(x) + g(x, \eta) \tag{11}$$

In above equation, White Gaussian noise refers to the model uncertainties.

$$f(x) = \begin{bmatrix} G(\sigma) \\ J^{-1}(-S(\sigma)J\omega + \tau) + J^{-1}(\tau_d) \end{bmatrix}$$

$$g(x) = \begin{bmatrix} 0_{3x1} \\ \eta_w \end{bmatrix}$$

η_w is the zero-mean White gaussian process The generalized Extended Kalman Filter equations are

$$\dot{\hat{P}} = F\hat{P} + \hat{P}F^T + GQG^T \tag{12}$$

Eq**??** and Eq12 are continuous-time state and covariance propagation equation, which are integrated through time to find their estimate.

$$\hat{x}_k^+ = \hat{x}_k^- + K_k y_k \tag{13}$$

$$\hat{P}_k^+ = [I - K_k H_k(\hat{x}_k^-)]\hat{P}_k^-[I - K_k H_k(\hat{x}_k^-)]^T + K_k R_k K_k \tag{14}$$

$$K_k = \frac{\hat{P}_k^- H_k^T(\hat{x}_k^-)}{[H_k(\hat{x}_k^-)\hat{P}_k^- H_k^T(\hat{x}_k^-) + R_k]} \tag{15}$$

where P is the state error covariance matrix,$\hat{x}_k^-$ is the predicted state at the discrete time instance k, $\hat{x}_k^+$ is the updated state at end of the k_{th} time instance,y_k is the residual measure, K_k is the Kalman gain . Eq14 gives the state covariance update at the end of the k_{th} time instance. Further,

$$F = \left.\frac{\partial f}{\partial x}\right|_{x=\hat{x}} = \begin{bmatrix} F_{11} & F_{12} \\ F_{21} & J^{-1}F_{22} \end{bmatrix} \tag{16}$$

$$F_{11} = \left(\frac{1}{2}\right)(\hat{\sigma}\hat{\omega} - \hat{\omega}\hat{\sigma}^T - S(\hat{\omega}) + \hat{\sigma}^T\hat{\omega}I_{3x3})$$

$$F_{12} = G(\sigma)$$

$$F_{21} = 0_{3x3}$$

$$F_{22} = \begin{bmatrix} 0 & -\omega_3 J_{22} + J_{33}\omega_3 & -\omega_2 J_{22} + J_{33}\omega_2 \\ \omega_3 J_{11} - J_{33}\omega_3 & 0 & \omega_1 J_{11} - J_{33}\omega_1 \\ \omega_2 J_{22} - J_{11}\omega_2 & -\omega_1 J_{11} + J_{22}\omega_1 & 0 \end{bmatrix}$$

$$G = \left.\frac{\partial g}{\partial \eta}\right|_{x=\hat{x}} = \begin{bmatrix} 0_{3x3} & 0_{3x3} \\ 0_{3x3} & I_{3x3} \end{bmatrix} \tag{17}$$

It is assumed that the measurements coming from the sensors provide us with MRP,σ, and angular velocity,ω, thus

$$h(x) = [\hat{\sigma}, \hat{\omega}]^T \tag{18}$$

$$H_k(\hat{x}_k^-) = \left.\frac{\partial H}{\partial x}\right|_{x=\hat{x}_k^-} = \begin{bmatrix} I_{3x3} & 0_{3x3} \\ 0_{3x3} & I_{3x3} \end{bmatrix} \tag{19}$$

If after propagating using Eq11, or, updating using Eq13, the magnitude of the MRPs is greater than unity,$\|\sigma\| > 1$, then the MRPs must be converted to their shadow set. Hence the state vector changes to

$$x^s = \begin{bmatrix} -\sigma/\sigma^T\sigma \\ \omega \end{bmatrix} \tag{20}$$

with this change, the covariance matrix for the shadow set also changes, which is defined in the terms of original set MRPs covariance matrix as

$$P^s = \begin{bmatrix} SP_{11}S^T & SP_{12} \\ P_{21}S^T & P_{22} \end{bmatrix} \tag{21}$$

$$P = \begin{bmatrix} P_{11} & P_{12} \\ P_{21} & P_{22} \end{bmatrix}$$

$$S = 2\sigma^{-4}\sigma\sigma^T - \sigma^{-2}I_{3x3}$$

where P is the state covarinace matrix of original MRP set and P^s is the state covariance matrix of the corresponding shadow set.Let the measured and estimated attitude at k_{th} time instance,t_k, be $\acute{\sigma}_k$ and $\hat{\sigma}_k$, respectively. Then the measurement residual can be defined as

$$y_k = \begin{bmatrix} y_{k1} \\ y_{k2} \end{bmatrix} \tag{22}$$

$$y_{k1} = \acute{\sigma}_k - \hat{\sigma}_k$$

$$y_{k2} = \omega_m - \hat{\omega}_k$$

where $\hat{\omega}_k$ is the estimated angular velocity and ω_m is the noisy measurement coming from the gyroscope. With MRPs, an ambiguity may arise while implementing EKF. As mentioned earlier, non-uniqueness of MRPs cause to have two representation for a single orientation, therefore, there is a possibility that the difference between measurement,$\acute{\sigma}_k$, and predicted MRPs,$\hat{\sigma}_k$, comes out larger for one set of MRPs and smaller for another.This kind of situation generally occurs around 180 orientation. [24] provides a subtle solution to this problem as an algorithm with following steps

$$For \quad y_{k1} = \acute{\sigma}_k - \hat{\sigma}_k$$

$$if\ \|\acute{\sigma}_k\| > 1/3, then$$

$$\check{y}_{k1} = \acute{\sigma}_k^s - \hat{\sigma}_k$$

$$if\ \|\check{y}_{k1}\| < \|y_{k1}\| then$$

$$y_{k1} = \check{y}_{k1}$$

$$endif$$

$$endif$$

IV. Non Linear Disturbance Observer

In this section, following [9], we have designed a nonlinear disturbance observer for the quadrotor model. From Eq8, we can write

$$\frac{d}{m} = \dot{v} + ge_3 - \frac{f_B}{m}(R(\sigma))^T e_3 \tag{23}$$

Let $\hat{d}$ be the estimated disturbance, then the observer dynamics can be written as

$$\dot{\hat{d}} = L(d - \hat{d}) \tag{24}$$

where L is the observer gain and it behaves such that if $\hat{d} > d$, then $\dot{\hat{d}} < 0$ and if $\hat{d} < d$, then $\dot{\hat{d}} > 0$.Using Eq22 and Eq23, we get

$$\frac{\dot{\hat{d}}}{m} = -L\left(\frac{\hat{d}}{m}\right) + L\left(\dot{v} + ge_3 - \frac{f_b}{m}(R(\sigma))^T e_3\right) \tag{25}$$

In the above equation, acceleration,$\dot{v}$, is not measurable and due to the noise in the measurement, its difficult to extract the same from the velocity signal. Therefore an auxiliary variable is defined as

$$z = \left(\frac{\hat{d}}{m}\right) - Lv \tag{26}$$

Differentiating Eq26 and using Eq25, we get

$$\dot{z} = \left(\frac{\dot{\hat{d}}}{m}\right) - L\dot{v} = -L\left(\frac{\hat{d}}{m}\right) + L\left(ge_3 - \frac{f_b}{m}(R(\sigma))^T e_3\right) \tag{27}$$

From Eq26, estimated disturbance is written as

$$\hat{d} = m(z + Lv) \tag{28}$$

Let $e(t)$ be the disturbance error defined as

$$e(t) = d - \hat{d} \tag{29}$$

differentiating above, we get

$$\dot{e(t)} = \dot{d} - \dot{\hat{d}} \tag{30}$$

Also, the considered disturbance varies slowly relative to the observer dynamics $\dot{d} \approx 0$. Therefore from Eq24, Eq29, and Eq30, we get

$$\dot{e} + Le = 0 \tag{31}$$

From Eq31 it can be shown that the observer is globally asymptotically stable by choosing Observer gain matrix L such that its diagonal elements are positive. In the similar manner, Non linear disturbance observer for inner loop is designed as follows

$$\dot{z_r} = -L_r\hat{\tau}_d + L_r(\omega \times J\omega - \tau)$$

$$\hat{\tau}_d = z_r + L_r J\omega \tag{32}$$

V. Controller Design

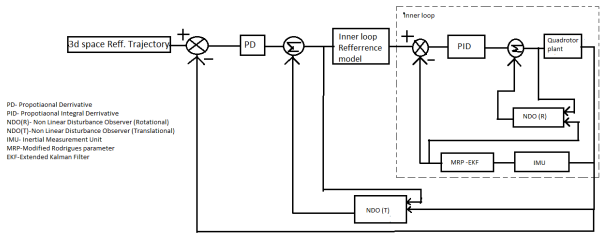

Fig. 2. Block diagram of the proposed control scheme

A. Outer loop control

In quadrotor, as discussed earlier, the outer loop functions in directing the thrust vector such that the quadrotor follows the desired spatial trajectory. The role of the inner loop controller is to maintain the orientation of the thrust vector, assigned by the outer loop. Fig2 shows the overall control scheme used in the quadrotor system. Considering p_d and v_d be the desired position and velocity, respectively, then error can be defined as

$$e_t = \begin{bmatrix}\tilde{p}\\ \tilde{v}\end{bmatrix} = \begin{bmatrix}p - p_d\\ v - v_d\end{bmatrix}$$

$$\dot{e}_t = \begin{bmatrix}\dot{\tilde{p}}\\ \dot{\tilde{v}}\end{bmatrix} = \begin{bmatrix}v - v_d\\ \dot{v} - \dot{v}_d\end{bmatrix} \tag{33}$$

Using Eq8 and Eq33, we get

$$\dot{\tilde{v}} = \dot{v} - \dot{v}_d = -ge_3 + \frac{f_B}{m}(R_d(\sigma_d))^T e_3 + \frac{d}{m} - \dot{v}_d \tag{34}$$

where $R_d(\sigma_d)$ represents the desired orientation of the quadrotor.Let U_t be defined as a control input for outer loop, then

$$U_t = \frac{f_B}{m}(R_d(\sigma_d))^T e_3$$

$$\dot{\tilde{v}} = -ge_3 + U_t + \frac{d}{m} - \dot{v}_d \tag{35}$$

The desired closed loop error dynamics, so that error asymptotically converges to zero

$$\dot{e}_t = -Ke_t$$

$$\begin{bmatrix}\dot{\tilde{p}}\\ \dot{\tilde{v}}\end{bmatrix} = -\begin{bmatrix}0_{3x3} & I_{3x3}\\ K_p & K_d\end{bmatrix}\begin{bmatrix}\tilde{p}\\ \tilde{v}\end{bmatrix} \tag{36}$$

where K is a $6x6$ gain matrix and K_pK_d are both positive.Using Eq35 and Eq36,we get

$$U_t = ge_3 - \frac{\hat{d}}{m} + \dot{v}_d - K_p\tilde{p} - K_d\tilde{v} \tag{37}$$

where $\hat{d}$ is the estimated disturbance coming from Eq28. To have a constrained control law, we can reformulate Eq37 as

$$U_t = ge_3 - \frac{\hat{d}}{m} + \dot{v}_d - \lambda_1 \tanh\left(K_p\tilde{p}\right) - \lambda_2 \tanh\left(K_d\tilde{v}\right) \tag{38}$$

where λ_1,$\lambda_2 > 0$. By selecting λ_1 and λ_2, we can have a control signal,U_t, of desired bound.

1) Stability analysis for outer loop: By substituting Eq38 and Eq36 in Eq35, we get the closed loop error dynamics as

$$\dot{e}_t = -\begin{bmatrix}0_{3x3} & I_{3x3}\\ K_p & K_d\end{bmatrix}e_t + \begin{bmatrix}0_{3x3}\\ I_{3x3}\end{bmatrix}\frac{\tilde{d}}{m} \tag{39}$$

where $\tilde{d} = d - \hat{d}$.Consider a lyapunov function V

$$V(t) = e_t^T P e_t \tag{40}$$

where P is a real symmetric positive deifinite matrix. Differentiating Eq40, we get

$$\dot{V(t)} = \dot{e_t^T} P e_t + e_t^T P \dot{e}_t \tag{41}$$

$$e_t^T P\dot{e}_t = e_t^T P\begin{bmatrix}0_{3x3}\\ I_{3x3}\end{bmatrix}\frac{\tilde{d}}{m} - e_t^T P\begin{bmatrix}0_{3x3} & I_{3x3}\\ K_p & K_d\end{bmatrix}e_t \tag{42}$$

$$\dot{e_t^T} P e_t = \frac{\tilde{d}^T}{m}\begin{bmatrix}0_{3x3} & I_{3x3}\end{bmatrix}Pe_t - e_t^T\begin{bmatrix}0_{3x3} & K_p\\ I_{3x3} & K_d\end{bmatrix}Pe_t \tag{43}$$

Let T be a positive-definite symmetric matrix defined by

$$T = \left(P\begin{bmatrix}0_{3x3} & I_{3x3}\\ K_p & K_d\end{bmatrix} + \begin{bmatrix}0_{3x3} & K_p\\ I_{3x3} & K_d\end{bmatrix}P\right)$$

then substituting Eq42 and Eq43 in Eq41, we get

$$\dot{V(t)} = -e_t^T T e_t + 2e_t^T P \begin{bmatrix} 0_{3x3} \\ I_{3x3} \end{bmatrix} \frac{\tilde{d}}{m} \tag{44}$$

The upper bound for $\dot{V(t)}$ can be defined as

$$\dot{V(t)} \leqslant -\lambda_{min}(T)\|e_t\|^2 + 2\lambda_{max}(P)\|e_t\| \frac{\left\|\tilde{d}\right\|}{m} \tag{45}$$

where λ_{min} and λ_{max} denote the minimum and maximum eigenvalues of a matrix, respectively. So to have derrivtive of lyapunov function negative, we can ensure the following condition

$$\left\|\tilde{d}\right\| \leqslant m\frac{\lambda_{min}(T)\|e_t\|^2}{2\lambda_{max}(P)\|e_t\|} \tag{46}$$

by choosing proper P and K. Hence for any bounded initial tracking error $e_t(0)$, $V(t)$ will decrease along with time.

B. Reference model for Inner loop

We aim to determine the desired set of MRPs for the inner loop controller such that the body thrust vector is in the direction of the outer loop control input vector. We are interested in determining σ_d in Eq35. The model given here is following the one as given in [31]. In Eq35, $\left\|(R_d(\sigma_d))^T e_3\right\| = 1$, therefore we can write

$$f_B = m\|U_t\| \tag{47}$$

Now definig unit vectors $\vec{a}$ and $\vec{b}$ as

$$\vec{a} = \frac{m}{f_B}U_t, \vec{b} = e_3 = \begin{bmatrix} 0 & 0 & 1 \end{bmatrix}^T \tag{48}$$

then the desired set of MRP for which thrust vector would be directed towards the outer loop control input vector,U_t is[**32**]

$$\sigma_d = \frac{\vec{a} \times \vec{b}}{\|\vec{a}\|^2 + \vec{a}^T.\vec{b} + \|\vec{a}\|\sqrt{2(\|\vec{a}\|^2 + \vec{a}^T.\vec{b})}} \tag{49}$$

In certain situations, there might be a possibility where the desired path of the quadrotor is below the current position of the drone. In that case, the z-component of the outer loop control input vector would become negative according to the control law defined in Eq37. If it gets more negative than -1, then the denominator in the Eq49 becomes invalid as the term under the root can not be negative. Moreover, it's not desirable for the drone to descent with faster acceleration than gravitational acceleration, therefore to have the outer loop control input vector always directed upwards following condition must satisfy

$$\frac{\hat{d(3)}}{m} + \dot{v}_d(3) + \lambda_1 + \lambda_2 < g \tag{50}$$

where $\hat{d(3)}$ and $v_d(3)$ refers to the z-component of their respective vectors. One can choose desired acceleration,$v_d(3)$, and parameters λ_1, λ_2, according to a rough guess of the boundedness of the disturbance in the z-direction present in the working environment of the drone and make sure the constraint inequality holds.For calculating first and second derivatives of the desired set of MRPs, we have adapted the command filter technique from [31],[12]. Let the dynamics of state vector $\begin{bmatrix} x_1 & x_2 \end{bmatrix}^T$ be given by second order differential equation

$$\dot{x}_1 = x_2$$

$$\dot{x}_2 = -2\zeta\omega_n x_2 - \omega_n^2(x_1 - \sigma_d) \tag{51}$$

where ζ and ω_n are damping ratio and frequency, respectively. We get the output from the command filter by having the following substitution

$$\sigma_c \equiv x_1 \qquad \dot{\sigma_c} \equiv x_2 \qquad \ddot{\sigma_c} = -2\zeta\omega_n\dot{\sigma_c} - \omega_n^2(x_1 - \sigma_d)$$

We express commanded angular velocity and angular acceleration as

$$\omega_c = G^{-1}(\sigma_c)\dot{\sigma_c}$$

$$\dot{\omega_c} = \dot{G^{-1}}(\sigma_c)\dot{\sigma_c} + G^{-1}(\sigma_c)\ddot{\sigma_c} \tag{52}$$

$$\dot{G^{-1}}(\sigma_c) = -G^{-1}(\sigma_c)\dot{G}(\sigma_c)G^{-1}(\sigma_c)$$

$$G(\sigma_c) = \frac{1}{4}[(1 - \sigma_c^T\sigma_c)I_3 + 2S(\sigma_c) + 2\sigma_c\sigma_c^T]$$

$$\dot{G}(\sigma_c) = \frac{8}{(1 - \sigma_c^T\sigma_c)^2}[\dot{\sigma_c}\sigma_c^T + \sigma_c\dot{\sigma_c}^T - \dot{\sigma_c}^T\sigma_c I_3 - S(\dot{\sigma_c})]$$

$$-\frac{16\sigma_c^T\dot{\sigma_c}}{(1 - \sigma_c^T\sigma_c)^3}[(1 - \sigma_c^T\sigma_c)I_3 - 2S(\sigma_c) + 2\sigma_c\sigma_c^T]$$

C. Inner loop

For the inner loop controller, we have designed a nonlinear PID control law. Although the integral action of the control law makes the steady-state error to zero, implementing a disturbance observer with it makes the controller more robust to exogenous disturbances. Let the MRPs defining the relative attitude between desired and actual orientation be defined as

$$\sigma_e = \frac{(1 - \sigma_c^T\sigma_c)\sigma - (1 - \sigma^T\sigma)\sigma_c - 2S(\sigma_c)\sigma}{1 + \sigma^T\sigma\sigma_c^T\sigma_c + 2\sigma_c^T\sigma} \tag{53}$$

The value of σ_e becomes infinite when the denominator in Eq53 becomes zero or close to zero. This behaviour can be avoided by switching σ to shadow set, σ^s, whenever the value of the denominator in Eq53 comes close to zero.Let $\delta\omega$ be the angular velocity error expressed in the body frame β

$$\delta\omega = \omega - R_e\omega_c \tag{54}$$

where R_e is defined as

$$R_e = I_3 - \frac{4(1 - \sigma_e^T\sigma_e)}{(1 + \sigma_e^T\sigma_e)^2}S(\sigma_e) + \frac{8}{(1 + \sigma_e^T\sigma_e)^2}S(\sigma_e)^T S(\sigma_e) \tag{55}$$

As our aim is to drive $\delta\omega$ and σ_e to zero, we define lyapunov function as

$$V_r(t) = \frac{1}{2}\delta\omega^T[J]\delta\omega + 2K_r\log(1 + \sigma_e^T\sigma_e) + \frac{1}{2}z^T[K_r]z \tag{56}$$

where z is defined as

$$z = \int_0^t (K_r\sigma_e + J\dot{\delta\omega})dt$$

$$= K_r \int_0^t \sigma_e dt + [J](\delta\omega - \delta\omega_{t-1}) \quad (57)$$

z expression will grow unbounded for any finite steady error. Therefore by forcing it's value to zero, steady state error will also converge to zero. Now, taking derivative of the lyapunov function, we get

$$\dot{V_r} = \delta\omega^T[J]\dot{\delta\omega} + \frac{4\sigma_e^T K_r \dot{\sigma_e}}{(1+\sigma_e^T\sigma_e)} + z^T[K_I]\dot{z} \quad (58)$$

where the middle expression can be reduced to a simpler form by using Eq3 and the following identity

$$\sigma^T G(\sigma) = \frac{(1+\sigma^T\sigma)}{4}\sigma^T \quad (59)$$

Thus,the middle expression becomes

$$\frac{4\sigma_e^T K_r \dot{\sigma_e}}{(1+\sigma_e^T\sigma_e)} = \frac{4\sigma_e^T G(\sigma_e) K_r \delta\omega}{(1+\sigma_e^T\sigma_e)} = \delta\omega^T K_r \sigma_e$$

Now substituting the above and Eq57 in Eq58, we get

$$\dot{V_r} = \delta\omega^T[J]\dot{\delta\omega} + \delta\omega^T K_r\sigma_e + z^T[K_I](K_r\sigma_e + [J]\dot{\delta\omega})$$

$$= (\delta\omega + [K_I]z)^T([J]\dot{\delta\omega} + K_r\sigma_e) \quad (60)$$

Considering $[\dot{Q}]$ to be a symmetric positive definite matrix, the desired derivative of a Lyapunov function, such that it remains negative, can be defined as

$$\dot{V_r} = -(\delta\omega + [K_I]z)^T[\dot{Q}](\delta\omega + [K_I]z) \quad (61)$$

Comparing Eq60 and Eq61, we get

$$[J](\dot{\omega} - \dot{\omega_c} + S(\omega)\omega_c) + K_r\sigma_e = -[\dot{Q}](\delta\omega + [K_I]z) \quad (62)$$

Now substituting Eq9 and Eq57 in Eq62, we get

$$\tau = -K_r\sigma_e - [\dot{Q}]\delta\omega - [\dot{Q}][K_I](K_r\int_0^t \sigma_e dt + [J](\delta\omega - \delta\omega_{t-1})) \quad (63)$$
$$+ S(\omega)J\omega - [J](S(\omega)\omega_c - \dot{\omega_c}) - \hat{\tau}_d$$

where $\hat{\tau}_d$ is the estimated disturbance, calculated using Eq32.

1) Stability analysis for inner loop: For proving asymptotic stability of the derived inner loop control law we need to state a theorem from[21].

Theorem: Assume there exists a Lyapunov function$V(x)$ of the dynamical system $\dot{x} = f(x)$. Let Ω be the non-empty set of state vectors such that

$$x \in \Omega \quad \Rightarrow \dot{V}(x) = 0$$

If the first k-1 derivatives of V(x), evaluated on the set Ω, are zero

$$\frac{d^i V(x)}{dt^i} = 0 \quad \forall \quad x \in \Omega \qquad i = 1, 2, .., k-1$$

and the k_{th} derivative is negative definite on the set Ω

$$\frac{d^k V(x)}{dt^k} < 0 \quad \forall \quad x \in \Omega$$

then the system $x(t)$ is asymptotically stable if k is an odd number.

Eq61 is negative definite only in terms of $\delta\omega$ and z. It only guarantees that ω,σ and z are stable and$((\delta\omega + [K_I]z)) \rightarrow 0$.Therefore, the derived control law promises local stability and not asymptotic stability. To check for asymptotic convergence, we calculate the higher order derivative of the lyapunov function. The first non - zero higher derivative evaluated at the set $\dot{V} = 0$ is

$$\dddot{V}(\sigma, \delta\omega + [K_I]z = 0) = -K^2\sigma^T([I]^{-1})[P][I]\sigma \quad (64)$$

As the above is negative definite, therefore according to the before mentioned theorem asymptotic stability is proved. Although the stated Lyapunov function, Eq56, doesn't remain differentiable when MRPs switching takes place, it remains continuous. Therefore the Lyapunov function monotonously decreases even after the switching takes place, and hence the stability proof is considered to be valid.

VI. When left at up-down orientation

While performing numerical simulation on various trajectories, we found that when the drone is left to fly in an up-down orientation, it crashes into the ground before its thrust generated by rotors can face upwards. Although we have proved the stability of the formed control law, it was evident that it lacked the performance metric. Even for initial orientations set at near 90 degrees away from the reference frame Z-axis, the drone traverses horizontally way too far from the desired path. We later comprehended that the clarification for such undesirable behavior was that for attitude past 90 degrees from the reference z-axis, the quadrotor's net thrust vector acted downwards that made quadrotor acceleration more negative than gravitational acceleration in the downwards direction. Before the quadrotor's net thrust vector could turn upward in the +z axis and counter its development in - Z heading, the drone crashes into the ground. An adaptive control law can be applied to tackle this kind of problem. In adaptive control law, control parameters get auto-tuned according to the operating point in the state vector space. But this method requires a separate mechanism for computing control parameters, which increases the computational burden. This motivated us to come up with a much subtle solution to this problem. In our control law, we added some pre-checking conditions, which checked the initial angular displacement, phi, between the body Z-axis and the inertial frame Z-axis. If it came out to be beyond 90 degrees, then making the thrust vector upwards becomes the priority. Therefore, for the initial conditions where the thrust vector is not in the upward direction, we first generate a torque about either x-axis or y-axis(of body frame) to make the drone's Z-axis direct upwards. The selection of axis for giving torque depends upon the initial orientation of the quadrotor. In our solution, we first calculate the position of all four rotors

in the inertial frame and then chose those two motors which have the least value of Z-coordinate for generating torque. In this way, we avoid unwinding phenomena and quickly direct the z-axis of the body frame in an upward direction. As soon as the z-axis of the body frame comes in the conic

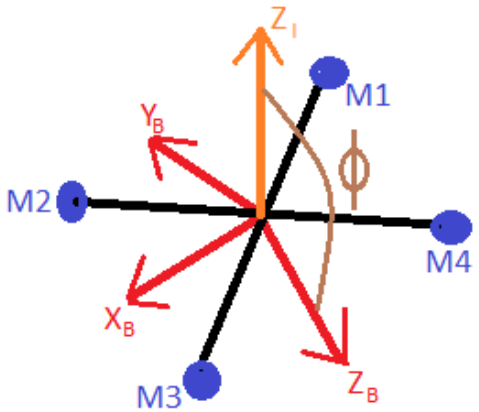

Fig. 3. Figure representing ϕ angle

section of certain cone angle made around the z-axis of the inertial frame, the nominal control law comes in action. The maximum thrust of each rotor limits the maximum amount of torque applied initially. This technique avoids the crashing into the ground and lessens the time of convergence between the actual trajectory and desired trajectory. The algorithm goes as follows:

1)First, we calculate the angle between the inertial frame z-axis and the body frame z-axis in the inertial frame: $\vec{m} = [0 \quad 0 \quad 1]^T$

$\vec{n} = R^T(\sigma)\vec{m}$

$$\phi = \frac{180}{\pi} \tan^{-1}\left(\frac{\|\vec{m} \times \vec{n}\|}{\vec{m}.\vec{n}}\right) \tag{65}$$

where $\vec{m}$ and $\vec{n}$ are representing Z-axis of the inertial frame and the body frame,respectively, in the inertial frame. Fig3 depicts a scenario were the thrust vector of the quadrotor is pointing in the downwards direction and where ϕ is the angle between the inertial Z-axis, Z_I, and the body Z-axis Z_B.

2)If ϕ measure comes out to be more than some specified value, in our case taken as 30 degrees, then find the motor coordinates in the inertial frame:

$$MC_B = \begin{bmatrix} -d & d & d & -d \\ d & d & -d & -d \\ 0 & 0 & 0 & 0 \end{bmatrix}$$

$$MC_I = R^T(\sigma)MC_B \tag{66}$$

MC_B and MC_I represents the motor coordinates in the body frame and the inertial frame, respectively.

3) Then we set the thrust of only those two motors which have least Z coordinate values.By doing so, we select that axis for applying torque,which will result in covering the least angular distance to attain the up-oriented thrust vector orientation. Let

$$T_m = rmg$$

whereT_m is the maximum thrust produced by the quad rotor and r is the thrust to weight ratio. The thrust to weight ratio for various classes of drones can be found in [4]. The thrust value of the motors is set according to the following law

$$F_i = \frac{\alpha T_m}{4} + \frac{(1-\alpha)T_m}{4}\frac{\phi}{180} \qquad 0 < \alpha < 1 \tag{67}$$

i=1,2 / 2,3 / 3,4 / 4,1

where α is a parameter varying between 0 and 1. At a single instance, i can take any two adjacent values out of the four options.These three steps are performed repetitively until the measure ϕ is less than some specified value(in our case 30 degrees). These steps are only initiated at the beginning of the flight.

VII. Result

We performed the numerical simulations in MATLAB software. Fig4 describes the parameters of the quadrotor model used in our simulations. An 8-shaped spatial trajectory is

m	0.429 Kg
d	0.1785 m
r	3.82
J_1	4.238 X 10^{-3} Kgm^2
J_2	4.986 X 10^{-3} Kgm^2
J_3	8.804 X 10^{-3} Kgm^2
c	0.03

Fig. 4. Quad rotor parameters

defined by the following equation

$$p_d = \begin{bmatrix} 5(1-\cos\left(\frac{\pi}{18}t\right)) \\ \sin\left(\frac{\pi}{9}t\right) \\ 10 \end{bmatrix} m$$

To simulate disturbances in the surrounding, following disturbances were modeled along and about the X,Y and Z axes.

$$d = \begin{bmatrix} 0.8\sin(0.1t) \\ \sin(0.1t) \\ 0.5\sin(0.1t) \end{bmatrix} N$$

$$\tau_d = \begin{bmatrix} 0.02\sin(0.1t) \\ 0.05\sin(0.1t) \\ 0 \end{bmatrix} Nm$$

Initial conditions at the start of the simulations were set at

$$p = [2, 2, 8]^T m, v = [0, 0, 0]^T m/s,$$
$$\omega = [0, 2\pi, 0]^T rad/sec, \sigma = [0, 1, 0]^T rad$$

The initial orientation,σ, can also be described as the 180 degree rotation about $y - axis$ of the quad rotor's body frame. This is calculated using relations between axis-angle, quaternions and Mrps. Our choice of taking initial orientation is such that the quadrotor's thrust vector faces downwards so that we can test our algorithm proposed in SectionVI. Outer loop and inner loop control parameters were set as following

$$K_r = 5I_{3x3}, \dot{Q} = 2I_{3x3}, K_I = 0.003I_{3x3}$$
$$\lambda_1 = 2.5, \lambda_2 = 2.5, K_p = 4, K_d = 3$$

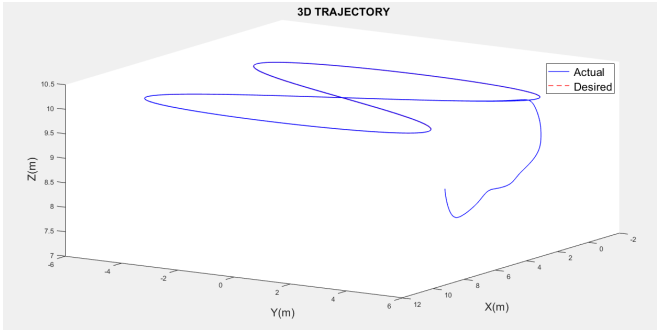

Fig. 5. 8-shape 3d-trajectory traversed by the quad rotor

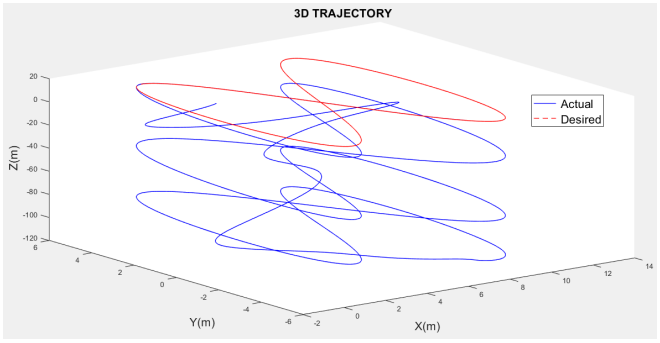

Fig. 6. 3d-trajectory traversed by the quad rotor without applying the algorithm proposed in section VI

Our results verify the efficacy of the proposed control law and the algorithm for handling orientations where the quadrotor's thrust vector is pointing downwards. Fig5 shows the resulting trajectory of the quadrotor in the 3d space. Fig5 and Fig9 infer that the quadrotor quickly rotates itself to make its thrust vector point upwards. While doing so, an advancement of around 50cm in (-)ve Z direction is evident in the graph. Fig10 and Fig6 corresponds to the z-plot and 3d-spatial trajectory for the case where the algorithm proposed in section VI is not applied. It is evident that the performance of the control law without the algorithm proposed in section VI is not desirable for initial orientations of quadrotor having

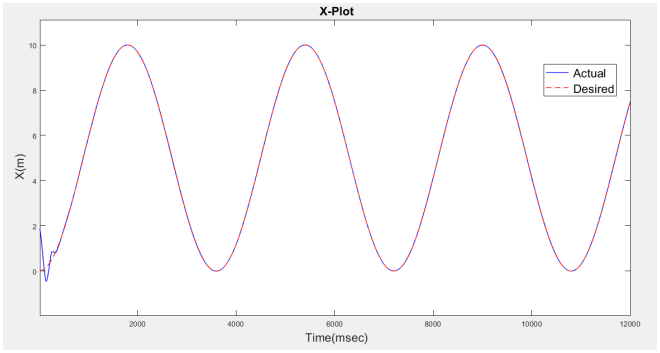

Fig. 7. X-Plot for the trajectory shown in Fig 5

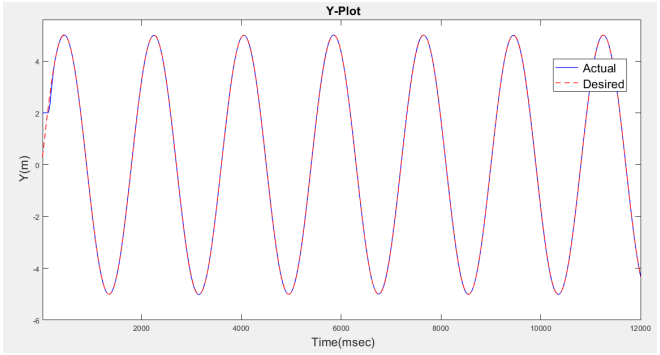

Fig. 8. Y-Plot for the trajectory shown in Fig 5

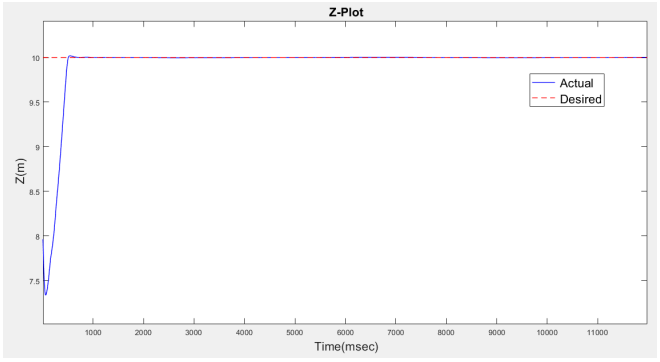

Fig. 9. Z-Plot for the trajectory shown in Fig 5

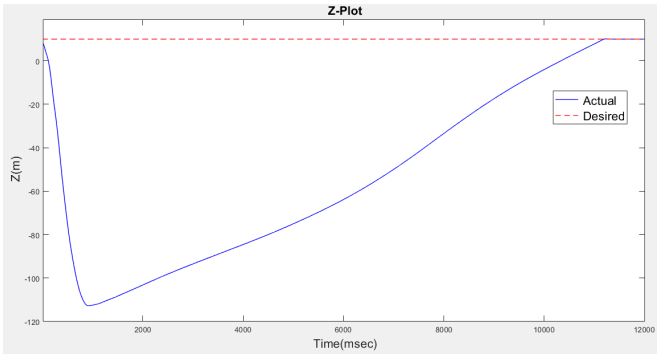

Fig. 10. Z-plot for the case where the algorithm proposed in Section VI is not applied

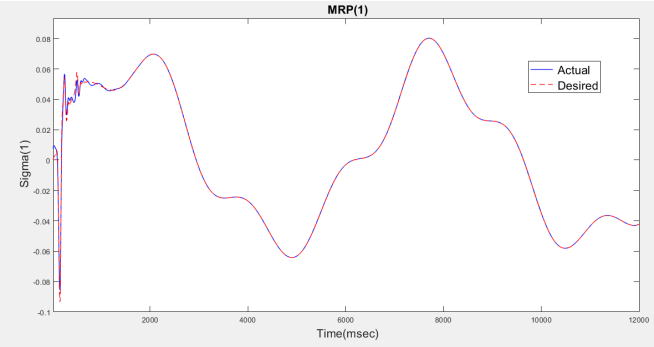

Fig. 11. First parameter of MRP

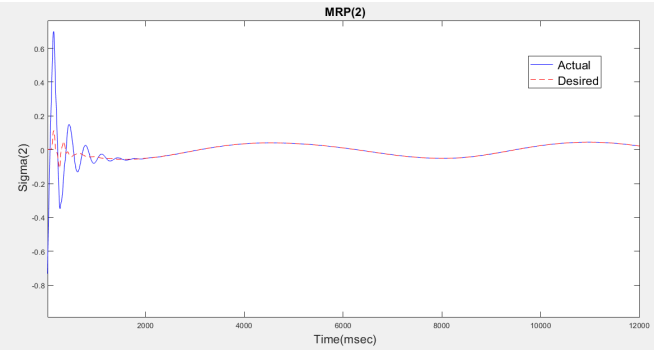

Fig. 12. Second parameter of MRP

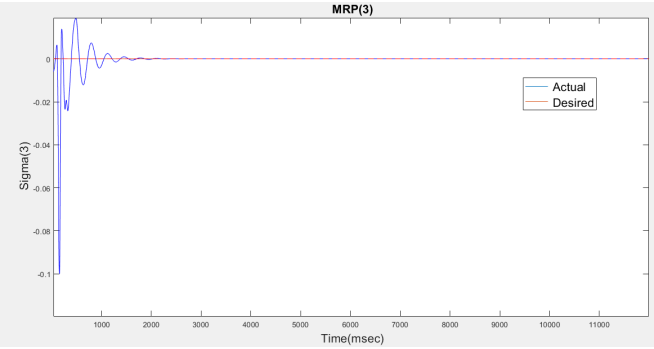

Fig. 13. Third parameter of MRP

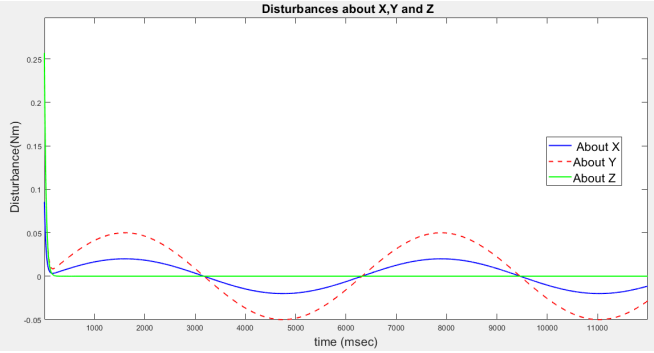

Fig. 14. Disturbances about X,Y and Z axes

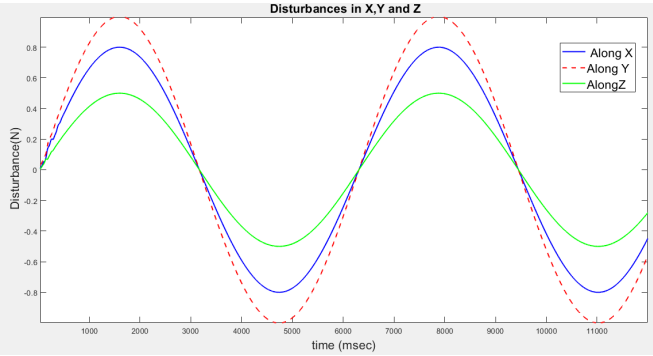

Fig. 15. Disturbances along X,Y and Z axes

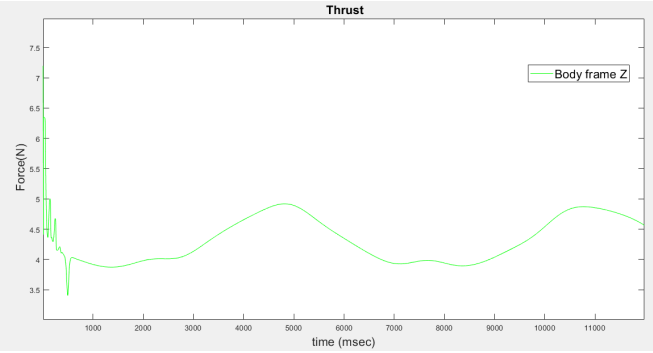

Fig. 16. Net Thrust magnitude

their thrust vectors pointed downwards. It can be seen in Fig10 that the actual Z value converges to the desired Z value after a significant amount of time.Thus, our proposed strategy helps in avoiding the undesirable horizontal advancements in the 3d space and makes quadrotor motion directed towards the desired trajectory in the least time. In Fig7, the actual plot, in blue, initially shows a wavy nature around the desired one(in red). The reason for the same is that the initial angular velocity of the quadrotor about the y-axis, makes the initial control torque to act also about the y-axis. This makes the advancement of the quadrotor in x-direction oscillating. Moreover, Fig12 and Fig13 show the waviness of the second and third parameters of the MRPs(representing rotation abut Y-axis and z-axis) at the initial stage, which is the direct consequence of the high initial angular velocity and control torque about Y-axis. Fig 14 and Fig15 shows the plot of estimated disturbances along and about the X, Y, and Z-axis, respectively. In Fig16, representing the net thrust of all four BLDC motors, initially, the magnitude of net thrust is very high due to the requirement of instant high torque to avoid undesirable horizontal advancements in the 3d space. Fig 17 and Fig18 represent the torque and the individual thrust of each BLDC motor, respectively.

VIII. Conclusion

This paper provides a robust global full degree of freedom, discontinuous trajectory tracking control. The use of a Nonlinear disturbance observer makes the control law robust

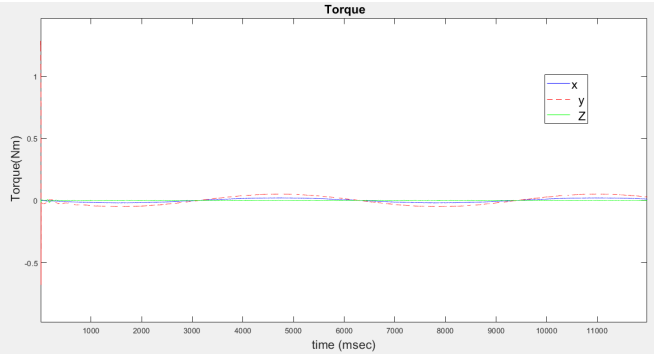

Fig. 17. Torque about X,Y and Z axes

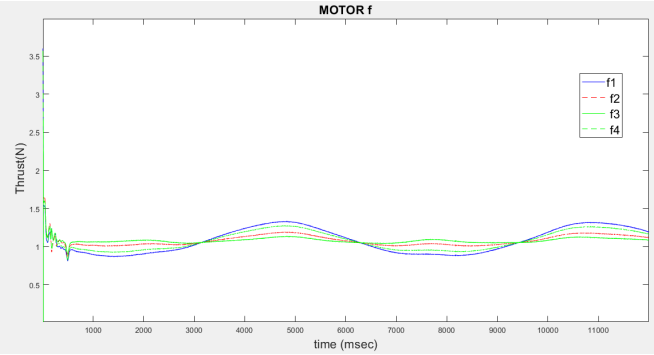

Fig. 18. Thrust force of each motor

against the slow varying exogenous disturbances. Additionally, EKF has been used to lessen the effect of the noises in sensor measurements and model uncertainties. Non-uniqueness property of the MRPs enables us to tackle the unwinding phenomena and deriving discontinuous, globally stable control law. We also provide a subtle technique to handle the up-down orientation of the quadrotor at the start of the flight, which makes the initial quadrotor take-off conditions more versatile. Finally, we have shown the simulation results to validate the proposed approach.

References

[1] Syed Muhammad Amrr, Sudipta Saha, and M. Nabi. "Anti-unwinding Robust Attitude Control of Spacecraft with Limited States Measurement". In: *2019 8th International Conference on Modeling Simulation and Applied Optimization (ICMSAO)* (2019). DOI: 10.1109/icmsao.2019.8880432.

[2] Pablo Bernal-Polo and Humberto Martınez-Barberá. "Kalman Filtering for Attitude Estimation with Quaternions and Concepts from Manifold Theory". In: *Sensors* 19.1 (Jan. 2019), p. 149. DOI: 10.3390/s19010149. URL: https://doi.org/10.3390/s19010149.

[3] S.p. Bhat and D.s. Bernstein. "A topological obstruction to global asymptotic stabilization of rotational motion and the unwinding phenomenon". In: *Proceedings of the 1998 American Control Conference. ACC (IEEE Cat. No.98CH36207)* (1998). DOI: 10.1109/acc.1998.688361.

[4] Marcin Biczyski et al. "Multirotor Sizing Methodology with Flight Time Estimation". In: *Journal of Advanced Transportation* 2020 (Jan. 2020), pp. 1–14. DOI: 10.1155/2020/9689604. URL: https://doi.org/10.1155%2F2020%2F9689604.

[5] Christian Bruccoleri and Daniele Mortari. "MRAD: Modified rodrigues vector attitude determination". In: *The Journal of the Astronautical Sciences* 54.3-4 (Dec. 2006), pp. 383–390. DOI: 10.1007/bf03256496. URL: https://doi.org/10.1007/bf03256496.

[6] Nathan Bucki and Mark W. Mueller. "A novel multicopter with improved torque disturbance rejection through added angular momentum". In: *International Journal of Intelligent Robotics and Applications* 3.2 (May 2019), pp. 131–143. DOI: 10.1007/s41315-019-00093-4. URL: https://doi.org/10.1007/s41315-019-00093-4.

[7] Jaeseung Byun, Simo A. Mäkiharju, and Mark W. Mueller. *A flow disturbance estimation and rejection strategy of multirotors with round trip trajectories*. 2020. eprint: arXiv:2003.02974.

[8] W. Chen, Q. Hu, and L. Guo. "Anti-unwinding attitude control of rigid spacecraft with angular velocity constraint". In: *2018 37th Chinese Control Conference (CCC)*. 2018, pp. 9776–9780.

[9] Wen-Hua Chen et al. "A nonlinear disturbance observer for robotic manipulators". In: *IEEE Transactions on Industrial Electronics* 47.4 (2000), pp. 932–938. DOI: 10.1109/41.857974.

[10] John L. Crassidis and F. Landis Markley. "Attitude Estimation Using Modified Rodrigues Parameters". In: 1996.

[11] HuTao Cui and XiaoJun Cheng. "Anti-unwinding attitude maneuver control of spacecraft considering bounded disturbance and input saturation". In: *Science China Technological Sciences* 55.9 (July 2012), pp. 2518–2529. DOI: 10.1007/s11431-012-4972-9. URL: https://doi.org/10.1007/s11431-012-4972-9.

[12] Jay A. Farrell et al. "Command filtered backstepping". In: *2008 American Control Conference* (2008). DOI: 10.1109/acc.2008.4586773.

[13] Christopher D. Karlgaard and Hanspeter Schaub. "Nonsingular Attitude Filtering Using Modified Rodrigues Parameters". In: *The Journal of the Astronautical Sciences* 57.4 (Oct. 2009), pp. 777–791. DOI: 10.1007/bf03321529. URL: https://doi.org/10.1007%2Fbf03321529.

[14] J. Kim, S. A. Gadsden, and S. A. Wilkerson. "A Comprehensive Survey of Control Strategies for Autonomous Quadrotors". In: *Canadian Journal of Electrical and Computer Engineering* 43.1 (2020), pp. 3–16.

[15] R. Lopez et al. "Disturbance rejection for a Quadrotor aircraft through a robust control". In: *2015 International Conference on Unmanned Aircraft Systems (ICUAS)*.

IEEE, June 2015. DOI: 10.1109/icuas.2015.7152317. URL: https://doi.org/10.1109/icuas.2015.7152317.

[16] Qi Lu, Beibei Ren, and Siva Parameswaran. "Uncertainty and Disturbance Estimator-Based Global Trajectory Tracking Control for a Quadrotor". In: *IEEE/ASME Transactions on Mechatronics* 25.3 (June 2020), pp. 1519–1530. DOI: 10.1109/tmech.2020.2978529. URL: https://doi.org/10.1109/tmech.2020.2978529.

[17] Jianting Lv, Dai Gao, and Xibin Cao. "Satellite attitude tracking control under control saturation". In: *2008 2nd International Symposium on Systems and Control in Aerospace and Astronautics*. IEEE, Dec. 2008. DOI: 10.1109/isscaa.2008.4776310. URL: https://doi.org/10.1109/isscaa.2008.4776310.

[18] Hamid Maqsood and Yaohong Qu. "Nonlinear Disturbance Observer Based Sliding Mode Control of Quadrotor Helicopter". In: *Journal of Electrical Engineering Technology* 15.3 (2020), pp. 1453–1461. DOI: 10.1007/s42835-020-00421-w.

[19] Christopher D. McKinnon and Angela P. Schoellig. "Estimating and reacting to forces and torques resulting from common aerodynamic disturbances acting on quadrotors". In: *Robotics and Autonomous Systems* 123 (Jan. 2020), p. 103314. DOI: 10.1016/j.robot.2019.103314. URL: https://doi.org/10.1016/j.robot.2019.103314.

[20] Amir Moeini, Alan F. Lynch, and Qing Zhao. "Disturbance observer-based nonlinear control of a quadrotor UAV". In: *Advanced Control for Applications: Engineering and Industrial Systems* 2.1 (Jan. 2020), e24. DOI: 10.1002/adc2.24. URL: https://doi.org/10.1002/adc2.24.

[21] Ranjan Mukherjee and Degang Chen. "Asymptotic stability theorem for autonomous systems". In: *Journal of Guidance, Control, and Dynamics* 16.5 (Sept. 1993), pp. 961–963. DOI: 10.2514/3.21108. URL: https://doi.org/10.2514%2F3.21108.

[22] M. Navabi and H. Mirzaei. "Robust Optimal Adaptive Trajectory Tracking Control of Quadrotor Helicopter". In: *Latin American Journal of Solids and Structures* 14.6 (June 2017), pp. 1040–1063. DOI: 10.1590/1679-78253595. URL: https://doi.org/10.1590%2F1679-78253595.

[23] Alexis Nez et al. "Identification of Noise Covariance Matrices to Improve Orientation Estimation by Kalman Filter". In: *Sensors* 18.10 (Oct. 2018), p. 3490. DOI: 10.3390/s18103490. URL: https://doi.org/10.3390/s18103490.

[24] Stephen A. O'Keefe and Hanspeter Schaub. "Shadow Set Considerations for Modified Rodrigues Parameter Attitude Filtering". In: *Journal of Guidance, Control, and Dynamics* 37.6 (Nov. 2014), pp. 2030–2035. DOI: 10.2514/1.g000405. URL: https://doi.org/10.2514/1.g000405.

[25] Mohamed Okasha, M. Idres, and Alia Abdul Ghaffar. "Satellite attitude tracking control using lyapunov control theory". In: *International Journal of Recent Technology and Engineering* 7 (Mar. 2019), pp. 253–257.

[26] Jitu Sanwale et al. "Quaternion-based position control of a quadrotor unmanned aerial vehicle using robust nonlinear third-order sliding mode control with disturbance cancellation". In: *Proceedings of the Institution of Mechanical Engineers, Part G: Journal of Aerospace Engineering* 234.4 (2019), pp. 997–1013. DOI: 10.1177/0954410019893215.

[27] Lu Wang and Heming Jia. "The Trajectory Tracking Problem of Quadrotor UAV: Global Stability Analysis and Control Design Based on the Cascade Theory". In: *Asian Journal of Control* 16.2 (June 2013), pp. 574–588. DOI: 10.1002/asjc.746. URL: https://doi.org/10.1002/asjc.746.

[28] Dunzhu Xia, Limei Cheng, and Yanhong Yao. "A Robust Inner and Outer Loop Control Method for Trajectory Tracking of a Quadrotor". In: *Sensors* 17.9 (2017), p. 2147. DOI: 10.3390/s17092147.

[29] Ahmad Bani Younes and Daniele Mortari. "Derivation of All Attitude Error Governing Equations for Attitude Filtering and Control". In: *Sensors* 19.21 (Oct. 2019), p. 4682. DOI: 10.3390/s19214682. URL: https://doi.org/10.3390/s19214682.

[30] Burak Yuksel et al. "A nonlinear force observer for quadrotors and application to physical interactive tasks". In: *2014 IEEE/ASME International Conference on Advanced Intelligent Mechatronics*. IEEE, July 2014. DOI: 10.1109/aim.2014.6878116. URL: https://doi.org/10.1109%2Faim.2014.6878116.

[31] Zongyu Zuo, Xiaofeng Ding, and Hao Liu. "Almost global trajectory tracking control of quadrotors with constrained control inputs". In: *Proceedings of the Institution of Mechanical Engineers, Part G: Journal of Aerospace Engineering* 230.5 (Aug. 2015), pp. 856–869. DOI: 10.1177/0954410015600461. URL: https://doi.org/10.1177%2F0954410015600461.